Eur Biophys J (2009) 38:1069–1078
DOI 10.1007/s00249-009-0511-4

ORIGINAL PAPER

Electromagnetic field (EMF) effects on channel activity of nanopore OmpF protein

M. Mohammadzadeh · H. Mobasheri · F. Arazm

Received: 5 March 2009 / Revised: 20 June 2009 / Accepted: 22 June 2009 / Published online: 15 July 2009

Abstract In this study, the effects of nonionizing electromagnetic fields (EMF; 925 MHz) on the OmpF porin channel have been characterized at the single-channel level. Channel activity was recorded in real time by the voltage clamp method. Our results showed an increase in the frequency of channel gating and voltage sensitivity. The effects of EMF lasted for several milliseconds after the field source was terminated. However, the conductance levels of channels did not change significantly. Thermal effects of EMF on single-channel properties are a possible cause, based on theoretical evaluation of results that were comparable to those seen in conventional experiments at different temperatures. We conclude that EMF affects both the dynamics and conformation of the channel, either directly by affecting critical amino acid side-chain arrangement, or indirectly, via the electrolyte or the lipid membrane.

Keywords Electromagnetic field (EMF) · Biophysics · Protein channel · Voltage clamp

Introduction

Biological effects of electromagnetic fields (EMF) have been the subject of many experimental and theoretical studies. High-frequency EMFs (100 KHz–10 GHz) including radio frequencies (RF) and microwaves have been examined to determine their thermal or nonthermal effects on biological systems. These investigations are particularly important in today's world, given that cordless and mobile telecommunication systems operate at 10 MHz–2 GHz, and their use may have implications regarding human health. Electrical appliances form constant and fluctuating charge gradients (Goodman et al. 1995) and spatial ion distributions both inside and outside living cells. Depending on their oscillating frequency, EMFs can affect cells in a thermal (Gandhi and Ross 1989; Foster and Glaser 2007) or nonthermal manner (de Pomerai et al. 2000; Bohr and Bohr 2000). The EMF evaluation factor, defined as specific absorption rate (SAR), is the only method currently available for measuring thermal and nonthermal effects of EMFs, and a more precise and targeted means of monitoring needs to be developed.

At the cellular level, exposure to EMFs has been shown to initiate a stress response within the cell (Richard et al. 2006). Different in vitro effects of EMFs on cells have been reported, including nonthermal effects on neuroblastoma (Dutta et al. 1992) and white blood cells (Chiang and Shao 1989). EMFs (10–1,000 GHz) cause resonant vibrational or rotational interactions in molecules, although this has not been observed at lower frequencies (Illinger 1981). EMFs are likely to initiate their effects via ion channels (Nonner and Eisenberg 2000) and receptors at the cell membrane. It is unclear whether they exert a direct effect on these proteins or they mediate through the immediate microenvironment. Both DC and AC electric fields (EF) (Farmer and Oman 1991; Barnes 2007) can result in structural effects across cell membranes. EMF has been shown to cause reorientation of membrane phospholipids and alteration of membrane potential subsequently

M. Mohammadzadeh · H. Mobasheri (✉)
Laboratory of Membrane Biophysics,
Institute of Biochemistry and Biophysics,
University of Tehran, PO Box 13145-1384, Tehran, Iran
e-mail: h.mobasheri@ibb.ut.ac.ir

F. Arazm
Communication Engineering Department,
Faculty of Computer and Electrical Engineering,
University of Tehran, Tehran, Iran

affecting channel behavior (Lindstrom et al. 1995). Diamagnetic characteristics of lipid clusters in the membrane are also enhanced in the presence of EMF. Although the lipid head-group area orientation remains intact, arrangement of hydrocarbon chains and lipid packing varies significantly (Gaber et al. 2005). The ultimate effect of EMF with high intensity is manifested as a conformational change occurring in biomacromolecules (Adair 2002; Tyazhelov et al. 1978) vulnerable to electric (Sharp and Honig 1990) and electromagnetic (Munoz et al. 2004) fields.

EMFs with different frequencies target biological matter at different levels. Low-frequency EMF disrupts ion diffusion while high-frequency EMF affects the molecular motion of water and intramolecular groups in macromolecules. Thus it is important to address the possible effect of the high-frequency EMF at the submolecular level. This necessitates a precise, fast, and noninterfering means of monitoring the EMF effect in the nanoenvironments in the vicinity of, or inside, the macromolecules.

Activity of single ion channels exposed to EMF experimentally demonstrates the way the applied EMF affects the dynamics of biological macromolecules in real time. For instance, exposing acetylcholine channels to EMF (10.75 GHz) decreases voltage sensitivity and increases open probability (d'Inzeo et al. 1988). Gramicidin A exposed to EMF (10 GHz) shows a nonthermal decline in channel formation, although conductance and half-life remain constant (Sandblom and Thenander 1991). In the presence of EMF, changes in membrane channels of brain cells cause changes in local ion concentration, osmotic pressure, cellular dehydration, and distortion of brain activity (Chiang and Shao 1989). EMFs from mobile phones have been shown to exert their side effects on membrane permeability, protein aggregation, and formation of amyloid fibrils nonthermally (De Pomerai et al. 2003) and on nerves and soft tissues thermally (Acar et al. 2009). Exposure to weak EMF results in few biological effects (Foster 2000), although some nonthermal effects (Adair 2003) have been reported. EMF (0.8 GHz) decreases conductance of the alamethicin channel by 15%, due to a rise in localized temperature, although this effect is reversible (Grigoriev and Pashovkin 2006).

All of the evidence thus far points to EMF-induced alterations in the microenvironment as a means of modulating ion channel and receptor activity. However, an oscillating field is theoretically capable of changing the activity of the voltage sensor group of a channel or receptor directly, thus affecting their gating state, sensitivity, and conductance proportionally to the magnitude and direction of the field (Cain 2005). It is most likely that, at high intensities, EMFs mediate their effects both directly and indirectly on ion channels and receptors. However, theoretical analysis has shown that EMF effects at low intensities are not strong enough to cause thermal effects in biological membrane, channels, and cells (Adair 2003). Although the structures of vital human membrane channels involved in signal transduction have not been fully resolved at the molecular level yet, the results of the current study conducted on a biological macromolecule might be used to define the path and tools required to study the EMF effects on VDAC1, Na–K channels, IP_3 receptors, and so on that may act as the most sensitive targets of EMF in humans.

In this study we have tried to determine the effects of low-intensity EMF at a single frequency of 925 MHz on the OmpF channel-forming protein whose structure is known at the atomic level and whose dynamics have been addressed in a great number of studies. Thus, the study will provide us with the detailed changes in the dynamics and structure of the channel caused by EMF at molecular level.

Materials and methods

The OmpF porin from *E.coli* K12 was kindly provided by M. Winterhalter and H. Weingart who extracted, purified, and used it for crystallography purposes based on the method published by Garavito and Rosenbusch (1986). Buffer used in these studies was $CaCl_2$ 10 mM, KCl 1M, HEPES 10 mM, pH 7.4. All chemicals were obtained from Sigma Chemical.

The reconstitution of the porin channel into the membrane occurs spontaneously at high protein concentrations, however, for incorporation of a single molecule, the concentration was lowered to a nanomolar level. Reconstitution was further facilitated by application of short pulses of high-voltage (±200 mV) potential differences (pds) that caused transient distortion of the membrane allowing channel incorporation. The activity of the channel in different membranes has been reported by different groups including Lakey and Pattus (1989). As the OmpF porin structure was compatible with the bilayer's physicochemical characteristics, the probability of reconstitution of the single trimeric channel pore into the bilayer was quite high. Reconstitution of a single channel was observed no more than 20 min after membrane formation and addition of porin protein to the chamber.

The protein was studied using an artificial bilayer system that was electrically isolated in a Faraday cage. Planar lipid bilayers were formed from soybean lecithin type II (Sigma). Briefly, bilayers were formed across a 50-μm-diameter hole in a PTFE septum (0.2 mm thickness) dividing a two-compartment glass chamber. The usual Teflon chamber in which the metal screws hold the blocks

together was not suitable for our experiment because the screws would act as a local antenna and would interfere with EMF irradiated by the main antenna. Consequently, we designed a single-piece glass chamber (4.5 cm long, 1.5 cm wide, and 1.5 cm high) that consisted of two compartments separated by a holed glass wall on which the PTFE Teflon sheet was mounted by means of silicon grease (Fig. 1a). The hole was made hydrophobic using 2 µl of coating solution, consisting of hexadecane in *n*-pentane 2% (V/V) followed by the formation of planar lipid bilayer based on the Montal and Muller technique (Montal and Mueller 1972). All recording parts of the set-up, including chamber, antenna, and preamplifier were located within a Faraday cage that was positioned on an air table.

EMF was produced by a signal generator (Wobbel Generator SWEEPGENERATOR WMC BN852, maximum output level of −3.4 dB) at a frequency of 925 MHz. EMF was applied perpendicular to the bilayer through two 1-mm-thick identical trapezoidal aluminum antennae, positioned in parallel, 5.5 cm apart from each other with the bilayer located in the middle. For calculation of electric field intensity at the location of membranes, the whole system was simulated by the High Frequency Structure Simulator (HFSS) program. The simulation results show homogeneity of the field at different locations, in particular in the vicinity of the membrane as defined in the 2D graph in Fig. 1b.

The strength of the field (intensity) caused by the applied field (E_0) is calculated by the finite element (FE) method used by the HFSS program. The input power of the signal generator P_w was calculated based on the following equation, where P_{out} (dB) is the output power of signal generator, −3.4 dB; L (dB) is attenuation of signal transmission line cable, 0.8 dB; A (dB) is the signal generator's gain; and G (dB) is the gain of the external amplifier. In our study, A (dB) and G (dB) are both set to zero.

$$P_w = 10^{\frac{P_{out}(\mathrm{dB}) - L(\mathrm{dB}) - A(\mathrm{dB}) + G(\mathrm{dB})}{10}} \times 0.001(\mathrm{W}) \quad (1)$$

Taking the output power of the signal generator to be 1 W, P_w was calculated based on Eq. 1. The actual value of the electric field sensed by the channel, E_{max}, can be determined from the value of E_0, calculated by the HFSS, according to Eq. 2 as follows:

$$E_{max} = E_0\sqrt{P_w} \quad (2)$$

The strength of the applied field irradiated perpendicular to the membrane, E_{max}, was found to be 244 V/m. If the membrane is situated perpendicular to the electric field, the actual field strength sensed by the protein can be estimated in a similar manner to be 4.76 V/m. Based on the above assumption and calculation, the input power would be −4.2 dB (0.38×10^{-3} W). Taking the dielectric constant to be $\varepsilon_0 = 8.854 \times 10^{-12}$ F/m and the magnetic permittivity of the medium to be $\mu_0 = 4 \times 3.14 \times 10^{-7}$ H/m, the impedance of free space based on Eq. 3

$$E/H = \sqrt{\frac{\mu_0}{\varepsilon_0}} \quad (3)$$

was calculated to be approximately 377 Ω (Stavroulakis 2003). Further, by assuming that the existing radiated wave at the membrane can be estimated by a plane wave, using the maximum strength of the electric field, E_{max}, we calculated the power density at the bilayer area based on Eq. 4:

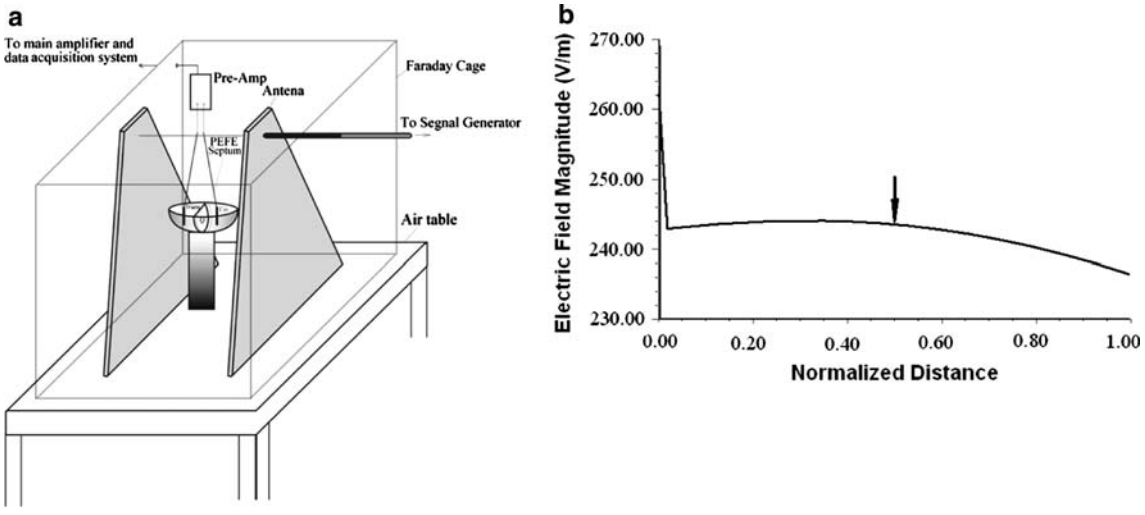

Fig. 1 The schematic representation of the set-up used for applying the EMF field to a single-ion channel. **a** Membrane area, recording chamber, antenna, Faraday cage, preamplifier, and antivibration air table. **b** The simulated graph has been normalized so that 1.00 corresponds to the distance between two antennas, 5.5 cm, and the *arrow* shows the plateau in the middle, where the membrane is located and the amplitude of the field is constant in its vicinity

$$S = \frac{E_{\max}^2}{2 \times 377} \quad (4)$$

where S is the power density in W/m^2, $E_{\max}$ is the maximum strength of the electric field in V/m, and the included value of 377 Ω represents the effects of the medium. Consequently, the power density caused by the applied EMF at the membrane location would be 0.03 W/m^2.

Data acquisition was carried out by the voltage clamp technique using an Adimi Filter Amplifier, digitized by CED 1401Plus (Cambridge Instruments), recorded and analyzed using a PC together with PAT 6 and PAT 7 software (J. Dempster, University of Strathclyde). The working compartment of the chamber that was connected to the virtual ground of the preamplifier was defined as the *cis* side. Channel activities were recorded at 20°C unless otherwise specified. Channel recordings were made using Ag–AgCl electrodes connected to agar bridges (1 mm diameter, agar 10 g/l in KCl 1 M). Sampling intervals were set to 500 μS, applied voltages ranged from ±10 to 300 mV, and the recording signal was filtered by two low-pass filters at 90 kHz. The membrane characteristics were evaluated at 120 Hz, 2 Vpp.

Channel-activity responses to EMF were monitored in different regimes: (1) in the presence of continuous EMF (cEMF), (2) recovering from EMF (rEMF) recorded after EMF was switched off, and (3) recovering from simultaneous application of EF and EMF (rcEMF). The results are based on the analysis of about 25 h of recordings at ±0 to 180 mV in 20-mV increments.

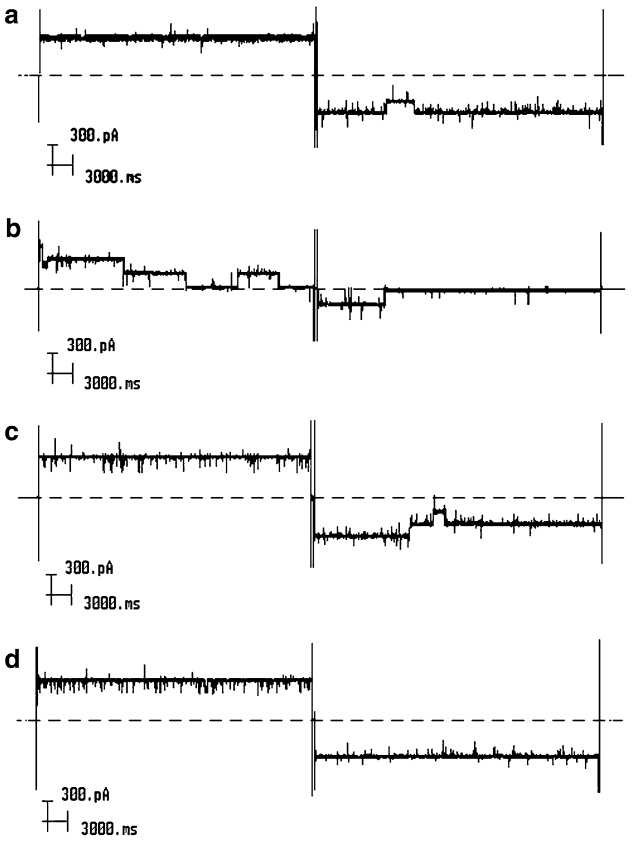

Fig. 2 The typical current traces of OmpF porin channels recorded in **a** the control group with no EMF applied and channels treated with EMF under different conditions: **b** cEMF, **c** rcEMF, and **d** rEMF at ±140 mV. *Broken line* represents the 0 pA current level. The *large vertical lines from left to right* represent the time when −ve pd, no pd, +ve pd, and no pd were applied, respectively. For detailed description of each condition, please see the text

Results

The stability of artificially formed planar lipid bilayers was assessed (± EMF) prior to each experiment through 17 sets of independent experiments for a total recording time of 170 min at 500-μS sampling intervals. Breaking voltage (voltage at which membrane is broken, V_b), capacitance (C_m) of the bilayer, and conductivity (G_m) at different polarities and potential differences were analyzed. There were no significant changes in membrane permeability observed at applied pds of up to ±200 mV at 20-mV increments in the presence and absence of EMF. In general, no significant changes in C_m, V_b, and G_m were identified.

OmpF channel activity in the control condition was consistent with published data (Fig. 2a). There were occasions when fast flickering was monitored at pds of ±80 to 130 mV. The voltage sensitivity of the channel increased significantly under cEMF conditions, so that at ±140 mV it completely closed at both positive and negative pds (Fig. 2b). Such a complete closure was rarely seen in the control group at 140 mV and was similar to what normally happens at 170–180 mV. In order to monitor the channel's recovery from the effects of combined EF and EMF, following the cEMF conditions, activity was recorded over a few milliseconds. Thus, through this approach, the channel activity was recorded while there was no EMF being applied. The channel under rcEMF conditions (Fig. 2c) still showed an increase in the voltage sensitivity but to a lesser extent. Channel activity that was recorded after applied EMF was terminated, rEMF, did not show a significant increase in voltage sensitivity (Fig. 2d). In most cases, both in the presence and absence of EMF, the channel showed more sensitivity to the positive pd applied to the *cis* side (where the negative current was produced) than negative polarity.

The current-to-voltage relationship of the channel at different field conditions was also studied to address the extent of the Ohmic relationship, the slope of changes in every monomer, and voltage sensitivity of the substates and monomers (Fig. 3). Increased gating appeared at lower pds whenever EMF was applied. Furthermore, the applied EMF

locked the channel at more intermediate states in cEMF, rcEMF, and rEMF groups. The voltage sensitivity of the channel highly increased in the cEMF group, showing complete closure at ±140 mV, and no sign of a fully open trimer at ±180 mV. The latter occurred in the rcEMF group only when −180 mV was applied. Complete closure in the rcEMF and rEMF groups, similar to the control group, took place at ±180 mV. The linearity and slope of the I/V line remained unchanged at pds up to ±140 mV before the closure of the fully open trimers formed the nonlinear part. The length of the linear part differed and could be ordered as follows: control > rEMF > rcEMF > cEMF (Fig. 3).

The main conductance of the channel under the different conditions cEMF, rEMF, and rcEMF showed no significant changes at different pds at both negative and positive polarities (Fig. 4). The graphs in Fig. 4 represent the conductance of the channel under control, cEMF, rEMF, and rcEMF conditions based on the activities of 17, 17, 3, and 3 separate membranes, each recorded for 170, 170, 30, and 30 min, respectively. However, substates were influenced by the applied EMF, and their long-lasting occurrences represented minor peaks or shoulders under cEMF, rEMF, and rcEMF conditions. The highest number of substates occurred in the rEMF group and was the same in the cEMF and rcEMF groups. Some recordings showed that with positive pd applied to the *cis* side, the voltage sensitivity in the presence of EMF increased and less stable and long-lived substates were formed (Fig. 4).

The thermal effect of EMF on channel activity was studied at temperatures of 22, 24, and 26°C, taking channel activity at 20°C as control (Fig. 2a). As significant change in activity was measured at 26°C, the corresponding results obtained at this temperature were compared with those recorded under cEMF (Fig. 5). It appeared that at 26°C, voltage sensitivity of the channel significantly increased, such that the complete closure occurred at much lower pds of ±160 mV (Fig. 5b). The actual closing events started at pds as low as ±80 mV. The channel showed an Ohmic behavior in all monomers at low voltages. The nonlinear part of the I/V curve started at pds as low as ±80 mV, where the first monomer in the fully open trimer closed. This voltage was ±140 for the second and ±160 mV for the last monomer. The conductance of the channel over the described temperature range did not show a significant difference from that of the control ($P < 0.05$) (Fig. 5c). However, there were more substates monitored, in particular when the fully open trimer was closing.

The probability of the channel being open when it was conducting through one monomer, two monomers (dimer), and three monomers (trimer) at ±160 and ±180 mV and at 20 and 26°C was compared to that of the probability under cEMF conditions at 20°C (Fig. 6). As shown, at 26°C the probability of channel activity in the fully open trimer state was lower than that seen for the dimer or monomer (Fig. 6b). There were rarely direct complete closures of the trimer; most closures went through dimeric or monomeric states. The higher the pds, the higher was the probability of complete closure in each monomer. As a result, the channel resided for a much shorter time (about 5% of total time) in the trimeric conducting state than in the dimeric (15%) or monomeric (25%) states. The occurrence of different channel states in the presence of cEMF showed a similar trend to that monitored at 26°C: the least time was spent

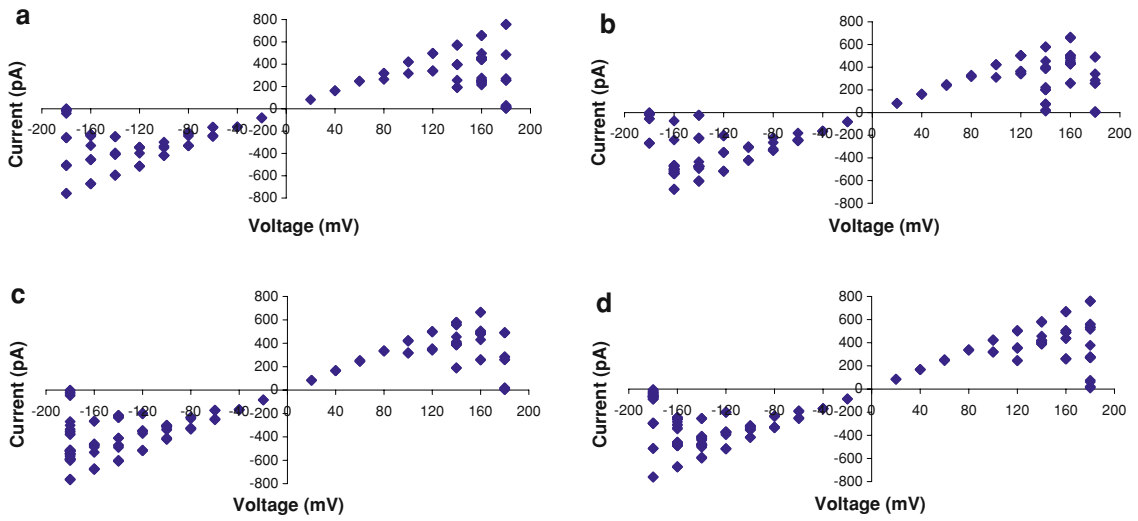

Fig. 3 The current-to-voltage relationship, I/V curve, of OmpF in **a** the absence of EMF taken as control group, and under different conditions: **b** cEMF, **c** rEMF, and **d** rcEMF groups. The main linear trends represent the Ohmic behavior of the trimer and voltage sensitivity of trimer, dimer, and monomers that form the nonlinear terminating part of the line. The higher voltage sensitivity of the channel under cEMF conditions has made several points at ±140 mV

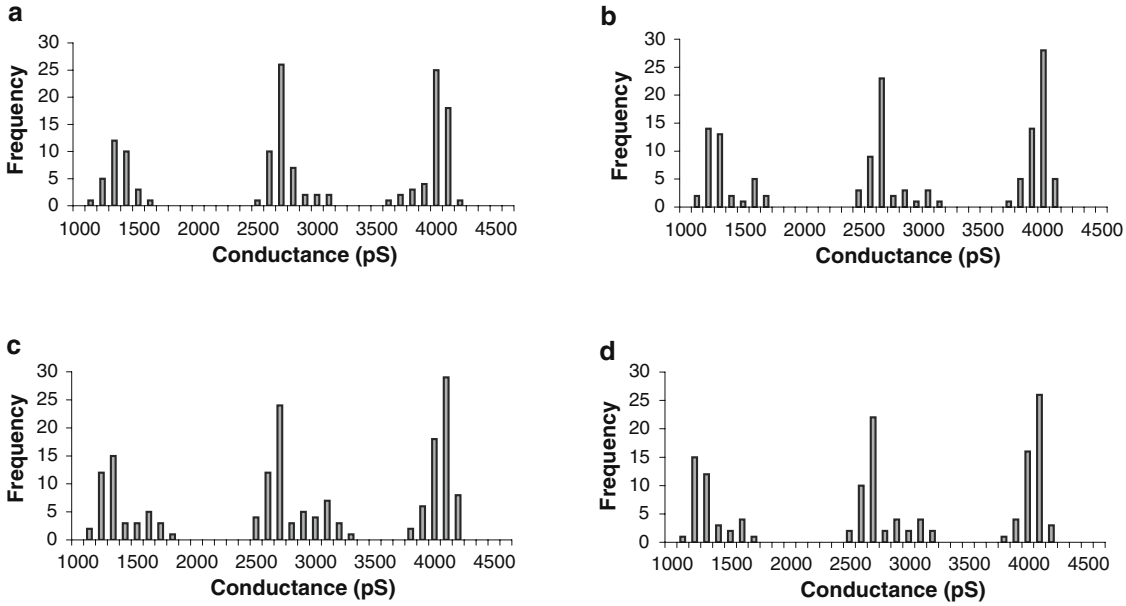

Fig. 4 OmpF channel conductances in the control group at 20°C in **a** the absence of EMF, and when it was treated with EMF under different conditions: **b** cEMF, **c** rcEMF, and **d** rEMF. The main states formed by OmpF monomers, dimers, and trimers together with the corresponding substates are shown. Bin size is set to 100

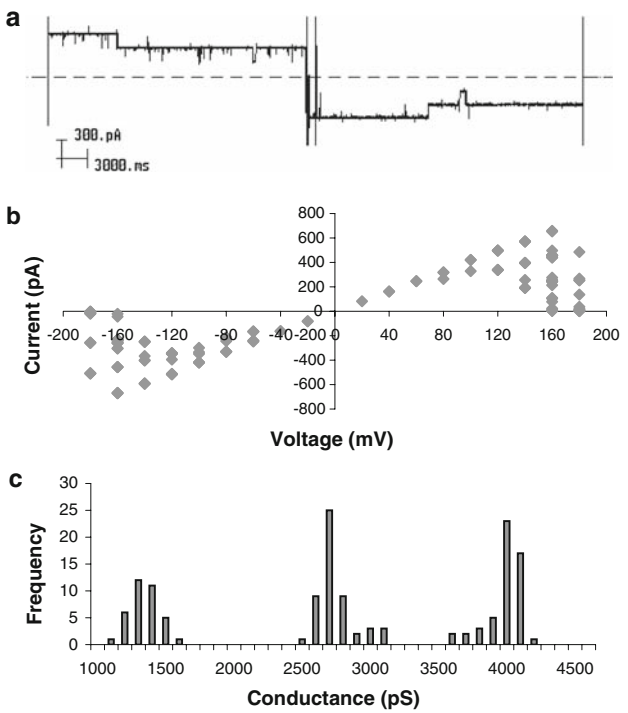

Fig. 5 The effects of a temperature of 26°C on the activity, voltage sensitivity, and conductance of the OmpF porin channel. The channel tended to close at lower voltages of ±140 mV (**a**), its I/V curve shows complete closure at ±160 mV with no trimer identified at ±180 mV (**b**), and more substates created at the trimer and dimer conductance levels (**c**)

conducting as a fully open trimer, more time as a dimer, and the longest time at the monomeric level. Proportionally, there was no significant difference between the time the channel spent in the fully closed state at 26°C and in the cEMF group, while the channel in both groups spent a much longer time closed than in the control group. In other words, compared with the control group recorded at 20°C, the duration of complete closure time of the trimer increased significantly, both at 26°C (Fig. 6b) and under cEMF conditions (Fig. 6c).

Discussion

In practice, it is difficult to monitor the effects of EMF at the molecular level in living cells or tissues. Molecular tracers, microscopic electrodes, and other means often interfere with EMF effects. It may be some time before the molecular dynamics of biological macromolecules in the presence of EMF can be monitored in real time at the molecular level. Consequently, the use of less-precise macroscopic approaches coupled with the complex behavior of living cells exposed to EMFs often results in controversial conclusions. Increasing evidence points to a relationship between nonlinear nonequilibrium processes and resonant responses in biomolecular systems, rather than equilibrium thermodynamics associated with thermal-energy exchanges and tissue heating (Adey 1993). EMF applied in this study exerts its effects at different sites

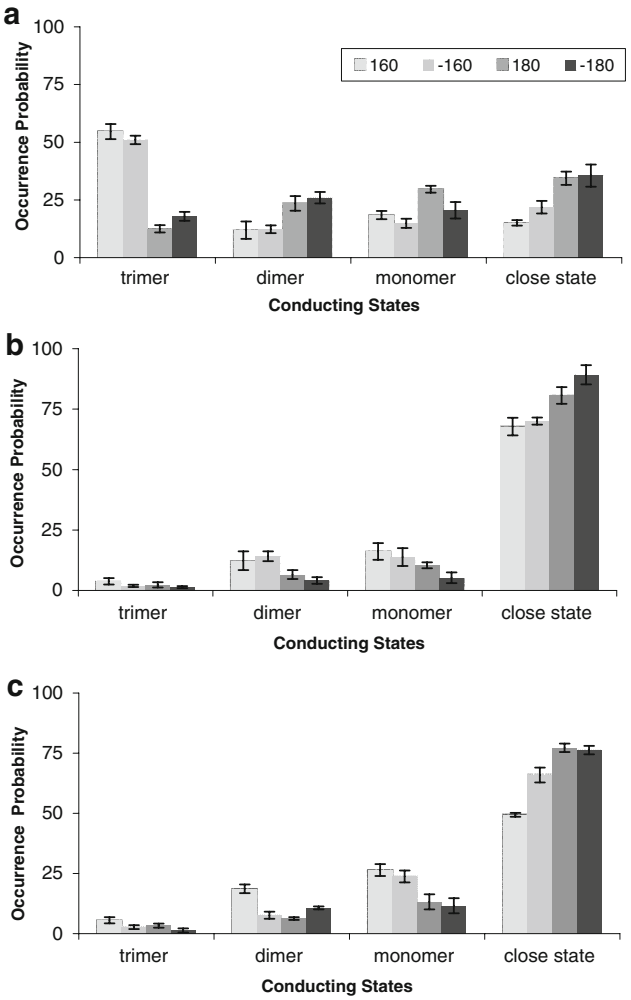

Fig. 6 Probability of the occurrence of trimer, dimer, monomer, and fully closed states in OmpF channel at 20°C (**a**), 26°C (**b**), and in the presence of cEMF at 20°C (**c**). Potential differences *from left to right* are +160, −160, +180 and −180 mV, respectively. The significant increase in closure probability and decrease in the occurrence of trimer, dimer, and monomer states at 26°C (**b**) and in the presence of cEMF at 20°C (**c**) are shown

including the hydrophobic core of the bilayer, the hydrophilic medium, and the macromolecule itself. As lipid phase transitions in membrane are reported to be caused by microwave exposure (Liburdy 1992), the changes in channel activity may be due to the effects of the applied cEMF on the packing of lipids and membrane viscosity.

The difference in the effects of rEMF and rcEMF copmared with those resulting from application of cEMF can be explained by membrane relaxation time, temperature diffusion, and reorganization. Oscillating electromagnetic fields have already shown some effects on membrane structure and function in synthetic liposomes and the lymphocyte cell membrane (Norden and Ramel 1992).

We did not observe a decrease in the conductance of the channel as reported for alamethicin (Grigoriev and Pashovkin 2006), possibly because of the differences in the structures of proteins studied and the nature of the field applied. If we consider the gating of the channel as the consequence of the transient conformation of the channel, as well as the lifetime of the structure profile and dynamics of the surrounding electrolytes at the gating area, this study shows that EMF harmonizes the molecular arrangements in favor of more stable substates. The EMF applied in this study caused the formation of stable substates, perhaps due to rearrangements of the side chains in the lumen of the channel. Alternatively, these substates may arise because of the reorientation and motion of ions and water molecules in the vicinity of the constriction zone.

Our results show that in the presence of EMF, the channel stays in the main open states for a much shorter time, in other words, the strain on the channel that dictates its dynamics has been partially compensated by the possible resonance and molecular motion caused by the EMF. This could be explained by the relaxation time of the voltage sensor region of the channel that has been addressed by applying an oscillating magnetic field (Cain 2005). Applying different combinations of EMF and EF—cEMF, rEMF, and rcEMF—resulted in different voltage sensitivities. In other words, the mechanism involved in the voltage sensitivity of channels was influenced by the EMF. The maximum effect was monitored when EMF was being applied, i.e., the cEMF condition, at the time of recording. The lower effects monitored under rcEMF showed that the channel could not recover and the condition caused under cEMF showed that it was lasting long enough to be monitored. However, the channel activity monitored in rEMF showed that it was the combination of EF and EMF that caused the changes in channel activity and that the channel recovered from the effects of EMF applied alone, if there were any, in a matter of milliseconds. Unfortunately, we were only able to monitor the EMF effects on the channel by voltage clamp studies, where the use of EF was unavoidable, otherwise, a fast and precise on-line spectroscopic experiment could show the role of EMF alone through the simultaneous application of EF in cEMF.

Considering the time scale and EMF conditions discussed above, we propose the changes in the oscillation potential of the charged groups involved in short-/long-range electrostatic interactions, hydration status, and orientation of side chains in the lumen of the channel as the main possible conditions distorted by applied EMF. The recovery time was about 10 ms in cEMF, lower in rcEMF, and even lower in rEMF groups. Thus, with regards to the lasting effects of EMF, our results show that the maximum effects are imposed when EF and EMF are applied simultaneously; this mimics the physiological condition where potential differences across the cell membranes keep cells hyperpolarized.

We conducted two sets of experiments to address the possible thermal effects indirectly. Our results showed, first, that the channel activity at 26°C was different from that monitored at 20, 22, and 24°C, and second, that the activity of the channel in cEMF was comparable with that of the control. Thus, we tried to compare the channel activity at 26°C with that monitored under cEMF (Fig. 5). To our surprise, the increased voltage sensitivity of the channel at 26°C was comparable to the cEMF condition. Further as in cEMF, the channel was so sensitive to the applied pd that the fully open trimer was not monitored at ±180 mV. Similarly, the closure events started at pds as low as ±80 mV and more substates were formed. We appreciate that the setting and monitoring of the macroscopic temperature of the medium cannot address the precise temperature and thermal motion happening in the nanoenvironment of the channel and in the vicinity of macromolecules. On the other hand, direct, rapid, and precise measurements of minute temperature changes in the nanoenvironment within, or in the vicinity of, the channel require technology that is not currently available.

Such an external means, if it exists, might itself interfere with the local thermal homogeneity of the field. There has been an atomic approach to address the thermal effect of microwaves in lysozyme crystals where the molecular dynamics of the protein has been reported in terms of the beta factor. X-ray diffraction study on tetragonal lysozyme crystals exposed to microwaves showed that, at low microwave power levels, the presence of the microwave field results in localized reproducible changes in the mean-square displacements (β factors). At particular sites, it is found that the β factors even decrease with increasing microwave power. It has been shown that the elevated temperature is due to the microwave absorption by unbound crystal water. The study shows no large microwave-driven displacements of structural subunits in the protein and claims that nonthermal effects do not appreciably alter the protein's structure and dynamics. Water damps resonant coupling of microwave fields to intramolecular vibrations, and it is therefore unlikely that proteins in the hydrated environment respond at high-frequency fields (several GHz), although nonresonant effects can alter protein structure and dynamics (Weissenborn et al. 2005).

The changes in the channel activity seen in this study could be due to a minor rise in localized temperature induced by the EMF microscopically. This phenomenon has been reported for the alamethicin channel (Grigoriev and Pashovkin 2006). Nonthermal RF field effects on GABA and acetylcholine receptors (D'Inzeo et al. 1988) and refolding of myoglobin (Mancinelli et al. 2004) have also been reported. This localized "hot spot" may be strong enough thermodynamically to disrupt hydrogen bonds and hydration states involved in gating and voltage sensitivity of the channel as well as conductivity of the area, causing structural rearrangement similar to that reported in thermophilic enzymes (Porcelli et al. 1997). An increase in temperature has been shown to increase the channel gating frequency (Hille 1984) consistent with what we observed during microwave exposure.

We also believe that changes in channel activity monitored in the presence of EMF might have been the result of indirect thermal/nonthermal effects on the bilayer. Microwave radiation has been reported to cause structural changes in acyl chain packing and increased disorder hydrolysis of carboxylic and phosphoric esters, conformational changes of the acyl chains, and even possible transient events in multilamellar vesicles (Gaber et al. 2005). We have not identified any particular conductance level(s) to represent newly formed pores. However, we suggest that the changes in channel activity correspond to changes in membrane packing and order, resulting in changes in membrane architecture that are capable of influencing reconstituted channel activity.

The EMF may have imposed thermal effects on different targets including the polar and hydrophobic residues in the channel-forming protein, membrane lipids, surrounding or intralumenal water, and conducting ions and their hydration state, such that we were unable to address them individually. Thus, what we monitored was the sum of all the effects on different targets including intermolecular motion of the channel, water motion within the channel and in the vicinity of the channel mouth on either side, as well as in the supporting lipid bilayer. The relaxation time represents the recovery of all of the mentioned targets following the removal of the field. Obviously, if we were able to monitor the effect on an isolated channel, then much shorter times would be required. In other words, the lipid bilayer and the surrounding electrolytes elongated the recovery time.

There is no doubt that the EMF characteristics can affect the gating frequency of the channel and the amplitude of the signal induced by the applied field (Galvanovskis and Sandblom 1997) leading to subsequent changes in the physicochemical condition of the cell due to changes in ionic flux. Bearing in mind the complexity of the biological systems and their electrical nature, it seems that evaluation of the biological effects of EMFs, solely based on the macroscopical measurements done in phantoms, is far from reality. Thus, faster, more sensitive, and precise data acquisition systems are required to monitor the possible changes in the structure and dynamics of biological macromolecules caused by the applied EMF in order to address their effects on molecular traffic through membrane, on the physicochemical condition of cells, and on cells' excitability and functional state.

In conclusion, through this study, we believe that for the first time a preliminary model has been developed to

measure the effects of EMF on single-channel properties. We appreciate the limitations of the system, i.e., failure to conduct rapid and precise measurements of temperature and conformational changes in the nanoenvironment within the channel lumen. This is why we are conducting a theoretical analysis of the data is necessary, to compensate for these shortcomings and to overcome experimental uncertainty in the description of the results of the practical experiments at the molecular level and to address the possible real condition and mechanism involved there indirectly. In the mean time, this study provides the basis for investigating the effects of EMF on mammalian single channels and may have implications in the context of human diseases.

Acknowledgments The authors appreciate the assistance of Eng Saeed Farsi for designing the antenna and simulating the EMF in the Faraday cage and chamber. We would also like to thank Dr. Edward Lea, University of East Anglia, and Dr. Edwin Thrower, Yale University, for their critical revision of the manuscript. The financial support of the University of Tehran is greatly appreciated.

References

Acar GO, Yener HM, Savrun FK, Kalkan T, Bayrak I, Enver O (2009) Thermal effects of mobile phones on facial nerves and surrounding soft tissue. Laryngoscope 119:559–562

Adair R (2002) Vibrational resonances in biological systems at microwave frequencies. Biophys J 82:1147–1152

Adair RK (2003) Biophysical limits on athermal effects of RF and microwave. Bioelectromagnetics 24:39–48

Adey WR (1993) Biological effects of electromagnetic fields. J Cell Biochem 51:410–416

Barnes FS (2007) Biological effects of magnetic and electromagnetic fields. Springer, London

Bohr H, Bohr J (2000) Microwave-enhanced folding and denaturation of globular proteins. Phys Rev E Sat Phys Plasmas Fluids Relat Interdiscip Topics 61(4):4310–4314

Cain CA (2005) Biological effects of oscillating electric fields: roles of voltage sensitive ion channels. Bioelectromagnetics 2(1):23–32

Chiang H, Shao BJ (1989) The effects of microwaves on the immune system in mice. Electromagn Biol Med 8:1–10

d'Inzeo G, Bernardi P, Eusebi F, Grassi F, Tamburello C, Zani BM (1988) Microwave effects on acetylcholine-induced channels in cultured chick myotubes. Bioelectromagnetics 9(4):363–372

de Pomerai D, Daniells C, David H, Allan J, Duce I, Mutwakil M, Thomas D, Sewell P, Tattersall J, Jones D, Candido P (2000) Non-thermal heat-shock response to microwaves. Nature 405:417–418

de Pomerai DI, Smith B, Dawe A, North K, Smith T, Archer DB, Duce IR, Jones D, Candido EP (2003) Microwave radiation can alter protein conformation without bulk heating. FEBS Lett 22;543(1–3):93–97

Dutta SK, Das K, Ghosh B, Blackman CF (1992) Dose dependence of acetylcholinesterase activity in neuroblastoma cells exposed to modulated radio-frequency electromagnetic radiation. Bioelectromagnetics 13:317–322

Farmer LE, Oman H (1991) Effects of DC and AC electric and magnetic fields on people and animals. IEEE 6:26–29

Foster KR (2000) Thermal and non thermal mechanisms of interaction of radio frequency energy with biological systems. IEEE Trans Plasma Sci 28:15–23

Foster KR, Glaser R (2007) Thermal mechanisms of interaction of radiofrequency energy with biological systems with relevance to exposure guidelines. Health Phys 92(6):609–620

Gaber MH, Abd El Halim N, Khalil WA (2005) Effect of microwave radiation on the biophysical properties of liposomes. Bioelectromagnetics 26:194–200

Galvanovskis J, Sandblom J (1997) Amplification of electromagnetic signals by ion channels. Biophy J 73:3056–3065

Gandhi CR, Ross DH (1989) Microwave induced stimulation of 32Pi-incorporation into phosphoinositides of rat brain synaptosomes. Radiat Environ Biophys 28:223–234

Garavito RM, Rosenbusch JP (1986) Isolation and crystallization of bacterial porin. Methods Enzymol 125:309–328

Goodman EM, B Greenebaum, Marron MT (1995) Effects of electromagnetic fields on molecules and cells. Int Rev Cytol 158:279–338

Grigoriev PA, Pashovkin TV (2006) Molecular mechanisms of microwave interactions with model ion channels. J Biol Phys Chem 6(4):163–165

Hille B (1984) Ionic channels of excitable membranes. Sinauer, Sunderland

Illinger KH (1981) Biological effects of nonionizing radiation. American Chemical Society Symposium Series no. 157. ACS, Washington DC

Lakey JH, Pattus F (1989) The voltage-dependent activity of Escherichia coli porins in different planar bilayer reconstitutions. Eur J Biochem 186(30):3–308

Liburdy RP (1992) The influence of oscillating electromagnetic fields on membrane structure and function. In: Norden B, Ramel C (eds) Interaction mechanisms of low-level electromagnetic fields in living systems. Oxford University Press, Oxford

Lindstrom T, Oksendal B, Ubøe J, Zhang T (1995) Stability properties of stochastic partial differential equations. Stoch Anal Appl 13:177–204

Mancinelli F, Caraglia M, Abbruzzese A, d'Ambrosio G, Massa R, Bismuto E (2004) Non-thermal effects of electromagnetic fields at mobile phone frequency on the refolding of intracellular protein:myglobin. J Cell Biochem 93:188–196

Montal M, Mueller P (1972) Formation of bimolecular membrane from lipid monolayers and a study of their electrical properties. Proc Natl Acad Sci USA 69(12):3561–3566

Munoz S, Sebastian JL, Sancho M, Miranda JM (2004) Transmembrane voltage induced on altered erythrocyte shapes exposed to RF fields. Bioelectromagnetics 25(8):631–633

Nonner W, Eisenberg B (2000) Electrodiffusion in ionic channels of biological membranes. J Mol Liq 87:149–162

Norden B, Ramel C (1992) Interaction mechanisms of low-level electromagnetic fields in living systems. Oxford University Press, Oxford

Porcelli M, Cacciapuoti GC, Fusco S, Massa R, d'Ambrosio G, Bertoldo C, De Rosa M, Zppia V (1997) Non-thermal effects of microwaves on proteins: thermophilic enzymes as model system. FEBS Lett 402:102–106

Richard HW, Funk T, Monsees K (2006) Effects of electromagnetic fields on cells: physiological and therapeutical approaches and molecular mechanisms of interaction. Cells Tissues Organs 182:59–78

Sandblom J, Thenander S (1991) The effect of microwave radiation on the stability and formation of gramicidin-a channels in lipid bilayer membranes. Bioelectromagnetics 12:9–20

Sharp KA, Honig B (1990) Electrostatic interactions in macromolecules: theory and applications. Annu Rev Biophys Biophys Chem 19:301–332

Stavroulakis P (2003) Biological effects of electromagnetic fields. Springer, Berlin

Tyazhelov VV, Alekseev SI, Grigor'ev PA (1978) Changes in the conductivity of alamethicin modified phospholipid membranes upon exposure to a high frequency electromagnetic field. Biofizika 23:732–733

Weissenborn R, Diederichs K, Welte W, Mareta G, Gisler T (2005) Non-thermal microwave effects on protein dynamics? An X-ray diffraction study on tetragonal lysozyme crystals. Acta Crystallogr D 61:163–172